

KINETICS OF HYDROGEN ABSORPTION IN GETTER MATERIALS FOR A CYLINDRICAL TANK: ANALYTICAL AND NUMERICAL RESOLUTIONS

GERMAIN GONDOR^a, RACHID LAYDI^b, CHRISTIAN LEXCELLENT^{a,*}

^a Institut FEMTO-ST, Département de Mécanique Appliquée,
Université de Franche-Comté

24 chemin de l'Epitaphe, 25000 Besançon, France

^b Ecole Nationale Supérieure de Mécanique et des Microtechniques (ENSMM),
Service Mathématique

26 chemin de l'Epitaphe, 25000 Besançon, France

* corresponding author: christian.lexcellent@univ-fcomte.fr

Abstract

The kinetics of hydrogen absorption in getter materials is studied. The dissociation of hydrogen molecules on the surface, penetration of hydrogen atoms into the material and bulk diffusion are taken into account. This paper extended the investigation on a wall (1D Cartesian case) performed by Liu et al. to a hollow cylinder more closed to technological application. The resolution of the equation system is solved in an analytical way (Bessel and Euler functions included) or by finite difference methods (Explicit and Implicit schemes are described). For a given time period, the filling rate of hydrogen absorbed in the container can be estimated.

Key words: kinetics, hydrogen storage, spectral methods, finite difference method

1. INTRODUCTION

Nowadays, a new challenge is to find and develop other alternative energy sources than petrol one which increases global warming of the earth. One solution can be the hydrogen storage. Hydrogen can be stocked in its gas state under high pressure (until 700 bar) but the problems of safety, mechanical efficiency of the tank must be solved. Another way can be the solid storage of hydrogen inside some intermetallics (Lanthanides, Magnesium...).

A layer of intermetallics can be also used as a getter material in an hybrid tank containing hydrogen gas under pressure. This paper will describe the kinetics of hydrogen absorption in a getter material. Chou et al. (2004) or Li et al. (2004) have described

the hydriding kinetics in an intermetallic compound ball using only bulk diffusion. Complementary to their analysis, three processes are taken into account in the present model: molecular dissociative chemisorption on the sample surface, atomic penetration from the surface to the bulk and diffusion in the body.

In fact, Liu et al (2004) solved the problem in one-dimensional situation for a wall (cartesian coordinates). We extend their investigation to the case of a hollow cylinder (cylindrical coordinates) for hydrogen storage.

The resolution of the system of equation is done by different ways. One part is devoted to analytical resolutions by the spectral method where the cases of Bessel and Euler functions are pointed out. An-

other part deals with a numerical resolution by finite difference method. Concerning this part, new explicit and implicit schemes taken into account boundary conditions are given for the finite difference method.

2. GETTER MODEL (LIU ET AL 2004)

At first, pumping H₂ gas by bulk getters involves dissociation of hydrogen molecule on the surface, penetration of hydrogen atoms into the materials as interstitials ones, and formation of H-metal compound in the form of a solid solution. The phase transformation associated to the hydride formation during the hydrogen storage (Schwarz and Khachaturyan 1995, 2006) is not taken into account in the present model.

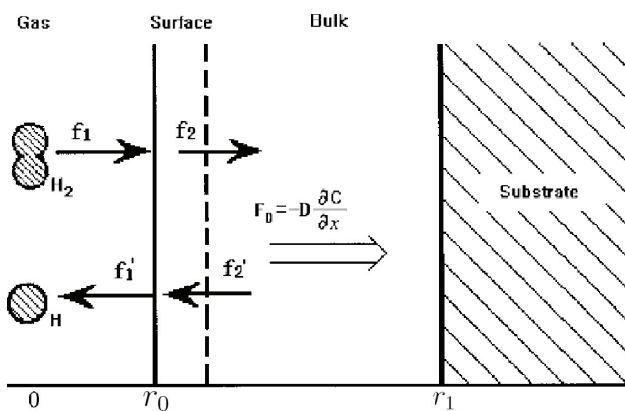
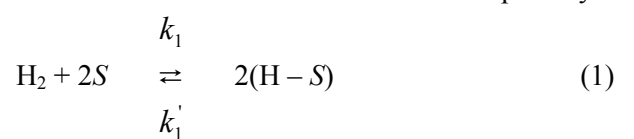


Figure 1. Schematic diagram of a bulk getter. f_1 - the incident flux of gaseous molecular hydrogen, f_1' - the flux of desorbing atoms, f_2 - the flux from the surface into bulk, f_2' - the backward flux from bulk to surface, r_0 - interior ray of the cylinder and r_1 exterior ray of the cylinder.

Here, in figure 1, one considers a cylindrical getter sample (r_0, r_1) which is mounted on a non-dissolving hydrogen substrate $r = r_1$. The surface $r = r_0$ is submitted to the gas pressure p_{H_2} .

2.1. Chemisorption

The interaction of a molecule H₂ with a metal surface is a typical chemical process. The energy of dissociation of H₂: E_{dis} of the order of 432 kJ/mol is smaller than the chemisorption energy which varies between 500 and 600 kJ/mol depending of the involved metal (Carter and Carnish, 2001). So a fraction of H₂ molecules hitting the surface will dissociate into two atoms H and becomes chemisorbed. The chemical reaction can be described in a simple way:



where S represents the absorbing site, k_1 , k_1' adsorption, desorption rates per unit surface area.

If θ stands for the surface coverage or the atomic fraction of H atoms on the surface, the incident molecular flux f_1 hitting on the surface can be expressed as:

$$f_1 = k_1(1 - \theta)^2 p_{H_2} \quad (2)$$

and the out-going atomic flux f_1' by :

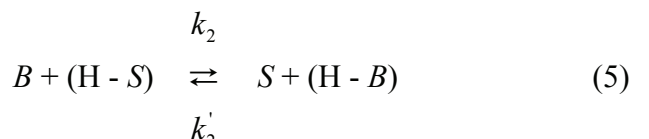
$$f_1' = k_1' \theta^2 \quad (3)$$

Hence, the rate of hydrogen dissociative chemisorption can be written as:

$$v_{chem} = k_1(1 - \theta)^2 p_{H_2} - k_1' \theta^2 \quad (4)$$

2.2. Penetration

The penetration of H atoms can be described by the expression:



where B vacant site in the subsurface layer
 $(H - B)$ the hydrogen atom dissolved in the matrix
 k_2, k_2' reaction constants in the forward and backward directions respectively

Let c_s the bulk atomic concentration near the surface. It can be considered as the hydrogen atomic concentration in the subsurface layer (number of hydrogen atoms per metal atoms).

In reference to figure 1, the penetration flux f_2 from the surface to the bulk can be written as:

$$f_2 = k_2 \theta (1 - c_s) \quad (6)$$

and the reverse flux :

$$f_2' = k_2' (1 - \theta) c_s \quad (7)$$



Hence, the transfer rate of hydrogen atom from the surface phase to the bulk is:

$$v_{pen} = k_2\theta(1 - c_s) - k'_2(1 - \theta)c_s \quad (8)$$

In the region near the surface layer, the sum of the flux is just balanced by the change of surface coverage:

$$\frac{d\theta}{dt} = k_1(1 - \theta)^2 p_{H_2} - k'_1\theta^2 - k_2\theta(1 - c_s) + k'_2(1 - \theta)c_s \quad (9)$$

Finally, when the surface and subsurface layer cannot dissolve hydrogen anymore $v_{chem} = v_{pen} = 0$, equilibrium between chemisorption, surface penetration and diffusion into the bulk is reached and hydrogen uptake in the getter is saturated. From eq (8), the saturated concentration $c_{s,max}$ in the subsurface layer is obtained under condition $v_{pen}(c_s = c_{s,max}) = 0$, it gives:

$$c_{s,max} = \frac{k_2\theta}{k'_2(1 - \theta) + k_2\theta} \quad (10)$$

During the surface chemisorption process, according to the Langmuir isothermal curve (Gao and Cui 1983), $v_{chem}(\theta, p_{H_2} = p_{eq}) = 0$, the surface coverage θ is given by :

$$\theta = \frac{\sqrt{K_1 p_{eq}}}{1 + \sqrt{K_1 p_{eq}}} \quad (11)$$

where p_{eq} is the equilibrium pressure of dissociation and $K_1 = k_1 / k'_1$. One has to note that the constant gas pressure p_0 applied in experiment is larger than p_{eq} . Generally, θ is determined by the chemisorption kinetics which depends on the getter material, absorbed gas, outer surface status and room conditions.

2.3. Diffusion

At low hydrogen content in the getter material, the spatial and the time behaviors of H atoms are characterized by the diffusion equation:

$$\frac{\partial c}{\partial t} = \Delta(Dc), \text{ and } t > 0 \quad (12)$$

with Δ is the Laplacian operator and t the time.

In 2D cylindrical coordinates with r the radius vector ($r \in]r_0, r_1[$):

$$\frac{\partial c}{\partial t} = D \left(\frac{1}{r} \frac{\partial c}{\partial r} + \frac{\partial^2 c}{\partial r^2} \right) \quad (13)$$

If no absorption occurs up to $t = 0$, the initial condition is:

$$c(r, t = 0) = 0 \quad (14)$$

Because the substrate does not dissolve hydrogen, the boundary condition at $r = r_1$ can be written as:

$$\left(\frac{\partial c}{\partial r} \right)_{r=r_1} = 0 \quad (15)$$

In the sub-surface layer of getter material (bulk phase), the H diffusion flux is determined by the penetration rate of atoms chemisorbed on the surface into the bulk. So the boundary condition at $r = r_0$ is:

$$-D \left(\frac{\partial c}{\partial r} \right)_{r=r_0} = k_2\theta(1 - c_s) - k'_2(1 - \theta)c_s \quad (16)$$

nd c_s represents c on the subsurface

Substituting equation (10) in equation (16), the boundary condition can be written as

$$-D \left(\frac{\partial c(r, t)}{\partial r} \right)_{r=r_0} = k_2\theta \left(1 - \frac{c_s}{c_{s,max}} \right) \quad (17)$$

Before solving the differential equation, a series of physical quantities must be normalized in terms of dimensionless parameters.

Let:

$$\lambda = \frac{r_0}{r_1} \text{ and } \Omega = [\lambda, 1] \quad (18)$$

$$\rho = \frac{r}{r_1} \text{ so } \rho \in \Omega \quad (19)$$

$$\tau = \frac{Dt}{r_1^2} \quad (20)$$

$$c'(\rho, \tau) = \frac{c(\rho, \tau)}{c_{s,max}} \quad (21)$$

The new system can be written as:

$$\frac{\partial c'}{\partial \tau} = \frac{1}{\rho} \frac{\partial c'}{\partial \rho} + \frac{\partial^2 c'}{\partial \rho^2} \quad (22)$$

$$c'(\rho, 0) = 0, \rho \in [\lambda, 1] \quad (23)$$



$$\left. \frac{\partial c'}{\partial \rho} \right|_{\rho=1} = 0 \quad (24)$$

$$\left. \frac{\partial c'}{\partial \rho} \right|_{\rho=\lambda} = -h(1 - c') \quad (25)$$

with $h = \frac{k_2 \theta r_i}{D c_{s,\max}}$ (26)

It is obvious that h almost covers all the important parameters of the hydrogen kinetics uptake. This parameter contains k_2 and θ involved in chemisorption kinetics, $c_{s,\max}$ and the diffusion coefficient D , which can be written, in a classical way, as :

$$D = D_0 \exp\left(-\frac{E_D}{RT}\right) \quad (27)$$

where E_D represents the bulk hydrogen diffusion activation energy in the intermetallic, R is gas constant and T stands for the temperature (in Kelvin degree).

The hydrogen quantity absorbed in the material can be estimated by

$$Q(\tau) = \int_{\Omega} c(\rho, \tau) d\rho \quad (28)$$

and the hydrogen rate absorption is delivered by

$$V_Q(\tau) = \frac{dQ}{d\tau} \quad (29)$$

3. RESOLUTION OF THE SYSTEM OF EQUATIONS

In such a system including the “Fick” diffusion equation with initial condition and boundary conditions, there are two ways of resolution. At first a research of some analytical solution and secondly the finite difference method can be used. We will develop these two methods and show that finally the obtained results are very closed.

For each case, for stability or homogeneity reasons, we decide to work on the complementary part of c' versus 1

$$\bar{c}(\rho, \tau) = 1 - c'(\rho, \tau) \quad (30)$$

The new system can be written as

$$\frac{\partial \bar{c}}{\partial \tau} = \frac{1}{\rho} \frac{\partial \bar{c}}{\partial \rho} + \frac{\partial^2 \bar{c}}{\partial \rho^2} \quad (\rho, \tau) \in \Omega \times [0, \infty[\quad (31)$$

$$\bar{c}(\rho, 0) = 1, \rho \in \Omega \quad (32)$$

$$\left. \frac{\partial \bar{c}(\rho, \tau)}{\partial \rho} \right|_{\rho=1} = 0 \quad \forall \tau > 0 \quad (33)$$

$$\left. \frac{\partial \bar{c}(\rho, \tau)}{\partial \rho} \right|_{\rho=\lambda} + h \bar{c} = 0 \quad \forall \tau > 0 \quad (34)$$

Laydi in (Laydi 2006) establishes some qualitative results:

- The problem solution \bar{c} is not negative
- The problem solution \bar{c} decreases with h decreasing
- The solution \bar{c} can be bounded by

$$0 \leq \bar{c} \leq \frac{1}{2} (1 + \lambda^{-1}) \exp(-\alpha \tau) \quad (35)$$

$$\alpha = 2(\gamma(1) - \gamma(\rho))^{-\frac{1}{2}} \quad (36)$$

With

$$\gamma(\rho) = \frac{\rho^4}{8} [4 - 5 \ln(\sigma \rho) + 2 \ln^2(\sigma \rho)] + \frac{\rho^2}{2} \left[\frac{1}{2} - \ln(\sigma \rho) + \ln^2(\sigma \rho) - 2\omega \right] \quad (37)$$

$$\sigma = \frac{1}{\lambda} \exp\left(\frac{1}{\lambda h}\right) \text{ and} \\ \omega = \lambda^2 \left(\frac{1}{2} - \ln(\sigma \lambda) + \ln^2(\sigma \lambda) \right) \quad (38)$$

This bounding solution proves that

$$\lim_{\tau \rightarrow \infty} \bar{c}(\rho, \tau) = 0, \forall \rho \in [\lambda, 1] \quad (39)$$

and

$$\tau \leq \frac{1}{\alpha} \ln\left(\frac{1}{2} \left(\frac{1 + \lambda^{-1}}{\bar{c}(\rho, \tau)} \right)\right) \quad (40)$$

Hence, for example, \bar{c} decreases by 50% (it means that hydrogen concentration c in the container increases by 50%) during a time maximum equal to:

$$\tau_{(1/2)} \leq \frac{1}{\alpha} \ln(1 + \lambda^{-1}) \quad (41)$$

3.1. Analytical investigation: spectral method

The spectral method is a classical one of variable separation (for instance τ and ρ) and permits to find the problem solution \bar{c} as a series:



$$\bar{c}(\rho, \tau) = \sum_{i=0}^{\infty} c_i(\tau) \psi_i(\rho) \quad (42)$$

where the functions $\{\psi_i\}_{i \in N}$ constitutes a basis of eigenfunctions of the second order differential operator on Ω . The ψ_i functions represent an orthonormal Hilbertian basis in $H_\zeta = L_2(\Omega)$ for the scalar product topology:

$$\langle u, v \rangle_\zeta = \int_{\Omega} \rho^\zeta u v d\rho \quad (43)$$

The problem is to find series

$\{(\psi_i, \eta_i)\}_{i \in N} \in H_\zeta \times R^+$ solution of the system (44):

$$\begin{cases} -\frac{d^2\psi_i}{d\rho^2} - \frac{1}{\rho} \frac{d\psi_i}{d\rho} = \eta_i \rho^{\zeta-1} \psi_i & \rho \in \Omega \\ -\frac{d\psi_i}{d\rho} + h\psi_i = 0 & \rho = \lambda \\ \frac{d\psi_i}{d\rho} = 0 & \rho = 1 \\ \langle \psi_i, \psi_k \rangle_\zeta = \delta_{i,k} & \forall k \in N \end{cases} \quad (44)$$

with δ the Kronecker matrix. Moreover, the system delivers:

$$\begin{cases} \sum_{i=0}^{\infty} \frac{dc_i}{d\tau} \langle \psi_i, \psi_j \rangle_1 + c_j \eta_j = 0 & \forall j \in N \\ c_j(0) = \langle 1, \psi_j \rangle_\zeta = g_j \end{cases} \quad (45)$$

Cutting out the equation of the system is possible only if $\langle \psi_i, \psi_j \rangle_{\zeta=1} = \delta_{i,j}$.

This case with $\zeta = 1$ corresponds to the Bessel equation but if the system resolution (44) can be processed in an explicit way, the calculation of eigenfunctions ψ_i is not trivial. Another useful case constitutes the Euler equations ($\zeta = -1$) where calculation of eigenfunctions is easy, but the system (45) is coupled.

3.1.1. Resolution with Bessel equations

In fact, with $\zeta = 1$, the system (45) becomes very simple:

$$\begin{cases} \frac{dc_j}{d\tau} + c_j \eta_j = 0 & \forall j \in N \\ c_j(0) = g_j \end{cases} \quad (46)$$

The solution is

$$c_j(\tau) = g_j \exp(-\eta_j \tau) \quad (47)$$

One has to indicate that ψ expression is well known:

$$\psi_j(\rho) = \gamma_j J_0(\sqrt{\eta_j} \rho) + \mu_j Y_0(\sqrt{\eta_j} \rho) \quad (48)$$

where J_ν is a first kind Bessel function of ν order and Y_ν a second kind Bessel function of ν order. But the boundaries conditions turn the calculations to be a little cumbersome and hence the determination of eigenfunctions.

3.1.2. Euler equations

As said previously, this choice corresponds to $\zeta = -1$:

$$\rho^2 \frac{d^2\psi_i}{d\rho^2} + \rho \frac{d\psi_i}{d\rho} + \eta_i \psi_i = 0 \quad (49)$$

The general solution is

$$\psi_i(\rho) = \alpha_{0,i} \sin(\sqrt{\eta_i} \ln(\rho)) + \alpha_{1,i} \cos(\sqrt{\eta_i} \ln(\rho)) \quad (50)$$

The calculation of eigenfunctions is very simple in comparison with the Bessel case:

$$\left(\frac{d\psi_i}{d\rho} \right)_{\rho=1} = 0 \Rightarrow \alpha_{0,i} = 0 \quad (51)$$

$$\left(\frac{d\psi_i}{d\rho} - h\psi_i \right)_{\rho=\lambda} = 0 \Rightarrow \frac{\sqrt{\eta_i}}{\lambda} [\sin(\sqrt{\eta_i} \ln(\lambda))] - h \cos(\sqrt{\eta_i} \ln(\lambda)) = 0 \quad (52)$$

The $\sqrt{\eta_i}$ values are obtained with the knowledge of the roots of the equation

$$\tan(z_i) = \frac{\beta}{z_i} \quad (53)$$

for $z_i = -\sqrt{\eta_i} \ln(\lambda) > 0$ and
 $\beta = -h\lambda \ln(\lambda) > 0$



The roots z_i are bounded

$$0 < z_0 \equiv -\sqrt{\eta_0} \ln(\lambda) < \frac{\pi}{2} \quad (54)$$

$$\frac{\pi}{2} + (i-1)\pi < z_i \equiv -\sqrt{\eta_i} \ln(\lambda) < \frac{\pi}{2} + i\pi \quad (55)$$

Lastly, $\forall i \in N$, one obtains:

$$\psi_i(\rho) = d_i^{-1/2} \cos(\sqrt{\eta_i} \ln(\rho)) \quad (56)$$

with

$$d_i = \frac{1}{2} \ln\left(\frac{1}{\rho}\right) + \frac{1}{4\sqrt{\eta_i}} \left(\sin\left(2\sqrt{\eta_i} \ln\left(\frac{1}{\rho}\right)\right) \right) \quad (57)$$

3.2 Finite difference method

3.2.1. Spatial discretization

Two discretizations are done, first a spatial one in Ω and further a temporal one in $[0, \tau]$.

Let $\rho_i = \lambda + i\delta_s$, $i = 0, \dots, n+1$ and $\delta_s = \frac{1-\lambda}{n+1}$

(figure 2)



Figure 2. Spatial discretization of the bulk getter

One has to examine the general conditions e.g. differential diffusion equation for $i = 1, \dots, n$ and the two boundary conditions: $i = 0$ on one side and $i = n+1$ on the other side.

In order to examine the general condition, the following operator is introduced:

$$L_i(\vec{c}) = \left(-\frac{\partial^2 \vec{c}}{\partial \rho^2} - \frac{1}{\rho} \frac{\partial \vec{c}}{\partial \rho} \right)_{\rho_i} \quad 1 \leq i \leq n \quad (58)$$

This result can be written in the mathematical form as:

$$\underline{\underline{A}}\vec{c} = L(\vec{c}) + \delta_s R_S(\vec{c}) \quad (59)$$

with R_S constitute a vector of residues and

$$\underline{\underline{A}} = \begin{pmatrix} \xi_1 & -\xi_1^- & -\xi_1^+ & 0 & \cdots & 0 \\ -\xi_2^- & \xi_2 & -\xi_2^+ & 0 & \cdots & 0 \\ 0 & \ddots & \ddots & \ddots & \ddots & \vdots \\ \vdots & \ddots & \ddots & \ddots & \ddots & 0 \\ 0 & \cdots & 0 & -\xi_{n-1}^- & \xi_{n-1} & -\xi_{n-1}^+ \\ 0 & \cdots & 0 & \xi_n^- & 0 & \xi_n \end{pmatrix} \quad (60)$$

represents the property of monotony. It means that $\underline{\underline{A}}^{-1}$ exists and $(\underline{\underline{A}}^{-1})_{(i,i)} \geq 0$. A table (table.1) can be given to explicit ξ_i , ξ_i^- and ξ_i^+ values:

Table 1. Table of constant for explicit and implicit schemes

	ξ_i^-	ξ_i	ξ_i^+
$i = 1$	$\frac{1}{\delta_s} \left(\frac{h}{2} + \frac{1}{\rho_1} \right)$	$\xi_1^- + \xi_1^+ + \frac{h}{2\delta_s}$	$\frac{1}{4\delta_s^2}$
$2 \leq i \leq n-1$	$\frac{1}{\delta_s^2}$	$\xi_i^- + \xi_i^+$	$\left(\frac{1}{\delta_s^2} + \frac{1}{\rho_i} \right) \frac{1}{\delta}$
$i = n$	$\frac{1}{4\delta_s^2}$	$\frac{1}{4\delta_s^2}$	\times

3.2.2. Temporal discretization

The temporal discretization can be carried out in an explicit or an implicit scheme. The adimensional temporal domain is $[0, \tau]$. Let be $\tau_j = j\delta_\tau$ with

$$\delta_\tau = \frac{\tau}{m+1} \quad (\text{figure 3}).$$

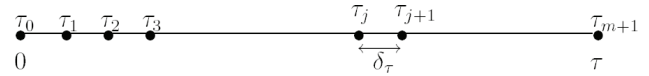


Figure 3. Temporal discretization of hydrogen absorption.

In an explicit scheme, the equation system is:

$$\left\{ \begin{array}{l} \vec{c}^{j+1} = (\underline{\underline{I}} - \delta_\tau \underline{\underline{A}}) \vec{c}^j \\ \vec{c}^0 = \vec{g} \end{array} \right. \quad \text{for each } j = 1, \dots, m \quad (61)$$

with $\underline{\underline{I}}$ the identity matrix and \vec{g} defined by (45). One can demonstrate a sufficient condition for the stability which is

$$\delta_\tau \leq \frac{\delta_s}{\frac{2}{\delta_s} + \left(h + \frac{1}{\lambda} \right)} \quad (62)$$

For an implicit scheme,

$$\left\{ \begin{array}{l} \vec{c}^{j+1} = \underline{\underline{D}} \vec{c}^j \\ \vec{c}^0 = \vec{g} \end{array} \right. \quad \text{for each } j = 1, \dots, m$$

$\underline{\underline{D}}$ must be calculated:

$$\underline{\underline{D}} = (\underline{\underline{I}} + \delta_\tau \underline{\underline{A}})^{-1} \quad (63)$$

This method is always stable without conditions for δ_s and δ_τ . In order to analyze the stability, it is sufficient to observe that



$$(\underline{I} + \delta_\tau \underline{A}) : \underline{1} \geq 1 \quad (64)$$

which gives

$$\|\underline{D}\|_\infty \leq 1 \quad (65)$$

$\|\underline{D}\|_\infty$ is the “spectral radius” and it can be demonstrated that this “spectral radius” is strictly inferior to one.

4. NUMERICAL SIMULATIONS AND COMPARISON BETWEEN THE DIFFERENT METHODS

4.1. Analytical and numerical simulation

In fact, to display numerical results, all analytical solutions are truncated at a finite value of n .

$$\bar{c}(\rho, \tau) \approx \sum_{i=0}^n c_i(\tau) \psi_i(\rho) \quad (66)$$

To simplify the number of variables, the number of spatial steps and temporal steps are equal to n

$$\delta_s = \frac{1-\lambda}{n+1} \text{ and } \delta_\tau = \frac{\tau}{n+1} \quad (67)$$

To analyze the convergence of analytical and numerical solutions, figure 4 presents the concentration for different values of n for $\lambda = 0.75$, $h = 1$ and $\tau = 0.5$. To estimate the value of the concentration, the set of equations (35) to (38) leads to $0.77 \leq c \leq 1$.

Calculations by the Euler method are significant for a truncated series with $n = 4$. Figure 4 shows that all plots with Euler method for $n = 4$ to $n = 256$ are on the same curve. Figure 4 displays convergence for the finite difference method with an implicit scheme. For $n \geq 32$ concentration is the same than the concentration given by the Euler method.

When convergence has occurred, the lower limit given by equations (35) to (38) are in good agreements with both simulations.

4.2. Concentration; amount and rate of hydrogen absorption

At given reduced time τ , if we examine the spatial evolution $\rho \in [\lambda = 0.75, 1]$ of the hydrogen concentration, for chosen values of h representing some ratio between surface penetration and bulk

diffusion, the low h ($h = 0.1$) value represents a predominance of diffusion while the high value $h = 10$ shows the reverse effect (figure 5). Then, when diffusion is high (h small), the concentration gradient is low and as a results the concentration is homogeneous. In the other case, the concentration on the inner boundary is bigger than on the outer one while the tank is not completely filled.

As an additive indication, the adimensional time necessary to reach an hydrogen storage equal to 90% of the saturated one are respectively 6.2, 0.74 and 0.33 for $h = 0.1$, $h = 1$ and $h = 10$.

The figure 6 shows the high h dependence of the amount of absorbed hydrogen Q as a function of $\sqrt{\tau}$. The figure 7 exhibits the rate absorption $V_Q(\tau)$ as a function of reduced time τ for different h values.

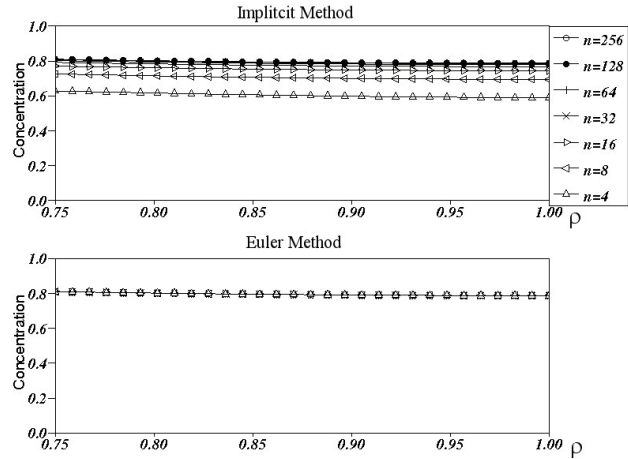


Figure 4. Evolution of hydrogen concentration C as a function of position ρ . (Effects of n)

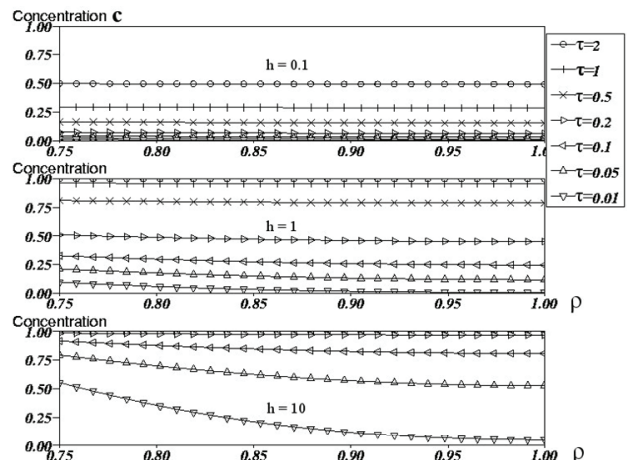


Figure 5. Simulation of the concentration for different of h and time τ calculated with Euler method and $n = 4$



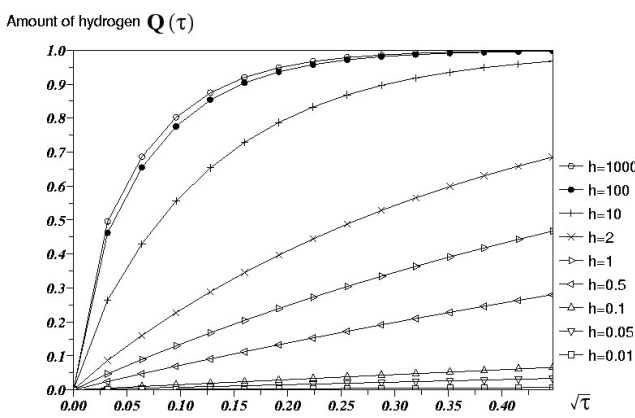


Figure 6. Amount of hydrogen for different values of h parameter calculated with Implicit method and $n = 64$

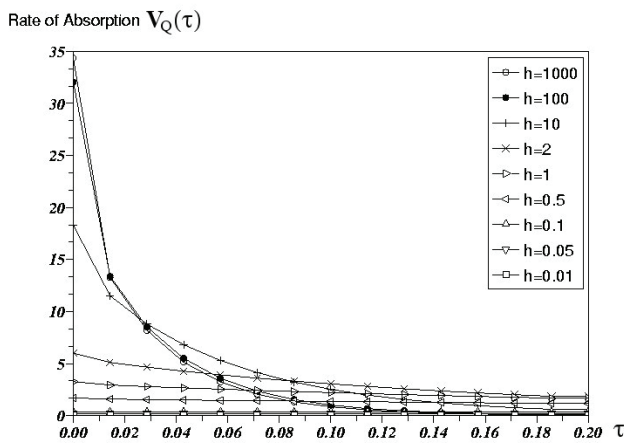


Figure 7. Rate of hydrogen absorption for different values of h parameter calculated with Implicit method and $n = 64$

5. CONCLUSION

A model of hydrogen storage in getter material developed by Liu et al. (2004) for a one dimensional cartesian situation has been extended with success for an hollow cylinder (*1D* axysymmetrical problem). A set of adimensional equations like "Fick" equation for diffusion plus boundary and initial conditions has been obtained. The system can be solved with analytical solutions using the spectral method or by finite difference method. For a sufficient number of terms of the analytical sum solution and a sufficient number of steps for the numerical one, solutions are close the ones to the others. The influence of the competition between surface penetration rate, and bulk diffusion rate (the h coefficient) has well been translated by the different curves evolution.

In the future, this work about the kinetics of hydrogen storage of containers must include the phase

transformation itself e.g. the hydride formation as Fernandez and Meyer (2000) initiate.

REFERENCES

- Carter, T.J., Cornish, L.A., 2001, Hydrogen in metal, *Eng. Fail. Anal.*, 8, 113-121
- Chou, K. C., Qian, L., Qin, L., Jiang, L. J., Xu, K. D., 2004, Kinetics of absorption and desorption of hydrogen in alloy powder, *Hydrogen Energy*, 30, 301-309.
- Fernández, G. E., Meyer, G., 2000, A reaction-diffusion analysis of the hydriding kinetics of zirconium-based alloys, *Journal of Nuclear Materials*, 279, 167-172
- Gao, B., Cui, S., 1983, *Vacuum physics*. Beijing: Scientific Press, 390 [in Chinese].
- Laydi, R, 2006, Private communication.
- Li, Q., Chou, K.C., Jiang, L.J., Feng, Z., 2004, Hydriding kinetics of the $\text{La}_{1.5}\text{Ni}_{0.5}\text{Mg}_{17}$ -H system prepared by hydriding combustion synthesis, *Intermetallics*, 12, 1293-1298.
- Liu, C.Z., Shi, L.Q., Xu, S.L., Zhou, Z.Y., Luo, Z.Y., Long, X.G, 2004, Kinetics of hydrogen uptake for getter materials, *Vacuum* 75, 71-78.
- Schwarz, R.B., Khachaturyan, A.G., 1995, Thermodynamics of open two-phase systems with coherent interfaces, *Physical Review Letters*, 74, 2523-2526.
- Schwarz, R.B., Khachaturyan, A.G., 2006, Thermodynamics of open two-phase systems with coherent interfaces: application to metal hydrogen systems, *Acta Materialia*, 54, 313-323.

KINETYKA ABSORPCJI WODORU W MATERIAŁACH POCHŁANIAJĄCYCH W CYLINDRYCZNYCH ZBIORNIKACH: ROZWIĄZANIE ANALITYCZNE I NUMERYCZNE

Streszczenie

W artykule opisano badania kinetyki absorpcji wodoru w materiałach pochłaniających. Rozważono dysocjację molekuł wodoru na powierzchni oraz wnikanie atomów wodoru do materiału i dyfuzję objętościową. Opisane badania rozszerzają wcześniejsze wyniki uzyskane przez Liu i in. dla płyty (przypadek Kartezjański 1D) na wnętrze cylindra, czyli przypadek bliższy zastosowaniom technologicznym. Rozwiążanie układu równań przeprowadzono analitycznie (za pomocą funkcji Bessela i Eulera) oraz metodą różnic skończonych (opisano schemat jawny I niejawny). W konsekwencji możliwe było określenie szybkości napełniania zbiornika wodorem w zadanym przedziale czasu.

Received: July 12, 2006

Received in a revised form: September 18, 2006

Accepted: September 20, 2006

